

Electronic Supplemental Information

Triple-Mode Tunable Long-persistent Luminescence in a 3D Zinc-Organic Hybrid

Yu-Juan Ma,^a Xiaoyu Fang,^a Guowei Xiao,^a Bo Lu^a and Dongpeng Yan^{*abc}

a. Beijing Key Laboratory of Energy Conversion and Storage Materials, College of Chemistry, Beijing Normal University, Beijing 100875, P. R. China. E-mail: yandp@bnu.edu.cn

b. Key Laboratory of Radiopharmaceuticals, Ministry of Education, Beijing Normal University, Beijing 100875, People's Republic of China.

c. College of Chemistry and Molecular Engineering, Zhengzhou University, Zhengzhou, 450001, China.

Contents

Experimental section

Figure S1. The coordination mode of D-Cam and tib.

Figure S2. Oscilloscope traces of SHG signals of KDP and **1**.

Figure S3. IR plot of **1**.

Figure S4. The prompt excitation spectra of **1** at room temperature.

Figure S5. The decay and IRF spectra of **1**.

Figure S6. The PL spectra (a) and CIE coordinate (b) of **1** at room temperature.

Figure S7. The temperature-dependent emission spectra of **1**.

Figure S8. The excitation wavelength-dependent emission spectra.

Figure S9. The delayed excitation spectra of **1** at room temperature.

Figure S10. (a) Prompt and delayed PL emission spectra of tib ($\lambda_{\text{ex}} = 307 \text{ nm}, 380 \text{ nm}$). (b) PL decay and fit curves obtained at room temperature.

Figure S11. (a) Prompt and delayed PL emission spectra of compound D-Cam ($\lambda_{\text{ex}} = 267 \text{ nm}, 310 \text{ nm}$). (b) PL decay and fit curves obtained at room temperature.

Figure S12. Phosphorescence spectrum of D-Cam and absorption spectrum of tib.

Figure S13. The delayed emission spectra (a) and CIE coordinate (b) of **1** at 77 K.

Figure S14. Time-resolved emission spectra.

Figure S15. (a) RTP decay at 525 nm and 535 nm of **1** (Insert: photo-activable process).

Figure S16. The temperature-dependent emission spectra.

Figure S17. (a) PL decay and fitting curves obtained at 77 K and (b) 327 K.

Figure S18. PXRD plot of **1**.

Figure S19. TG plot of **1**.

Figure S20. Calculated molecular orbitals.

Table S1. Crystallographic data for **1** at 100 K.

Table S2. Selected bond lengths (Å) and angles (°) for **1** at 100K.

Table S3 Phosphorescence lifetimes (τ) of **1**.

Experimental Section

Materials and methods

All chemicals were reagent grade and used as purchased without further purification.

Synthesis of 1: Zn(NO₃)₂·6H₂O (0.09g, 0.30 mmol), D-Cam (0.03 g, 0.15 mmol), tib (0.027g, 0.10 mmol) was added to mixed solution of 14 mL water and 1 mL DMF with a drop of concentrated HNO₃, then sealed in a Teflon-lined autoclave (20 mL) and heated to 140 °C for 3 days, colorless crystals were obtained and washed with deionized water. Yield: ca. 31% based on tib. IR of **1** (KBr pellets, cm⁻¹): 3422(s), 2963(w), 2876(w), 1605(s), 1508(s), 1385(s), 1287(m), 1242(m), 1076(s), 1018(m), 943(m), 872(m), 766(m), 687(m), 652(s), 536(w), 446(w).

The SHG measurements of the crystals samples were completed by a Nd:YAG laser with 1064 nm as fundamental frequency light. IR spectra was recorded on a Shimadzu IRAffinity-1 FT-IR spectrometer with KBr pellet. All luminescence data were measured on an FLS 980 fluorescence spectrometer. The absorption spectra were carried out on a Puxi Tu-1901 spectrophotometer with BaSO₄ reference. Thermogravimetric (TG) analysis was measured using a powder sample with a heating rate of 10°C K⁻¹ under N₂ atmosphere on a METTLER TOLEDO Thermogravimetric Analyzer. Powder X-ray diffraction (PXRD) data were recorded on a Shimadzu XRD-7000 (3KW) X-ray diffractometer. Simulated curve of PXRD was exported by the single-crystal data and diffraction-crystal module of the Mercury (Hg) program available free of charge *via* the Internet at <http://www.iucr.org>.

X-ray Crystallography.

The single-crystal X-ray diffraction data of **1** was collected on a Rigaku XtalLAB Synergy diffractometer at 100(10) K with Cu-K α radiation ($\lambda = 1.54184 \text{ \AA}$). SHELX-2016 software was used to solve and refine the structure.¹ Crystallographic data for **1** are listed in Table S1, and selected bond lengths and angles are listed in Table S2. Full crystallographic data for **1** has been deposited with the CCDC (2079214).

Calculation Details

All DFT calculation were carried out with the D.01 revision of the Gaussian 09 program package², using the cam-b3lyp functional with the 6-311G* basis set for C, H, O and N, and lanl2dz basis set for the Zn element. The D3 Grimme's dispersion term with Becke-Johnson damping was added to the cam-B3LYP functional to get a better description of the intramolecular non-covalent interactions. In this work, the frontier orbitals were analyzed by Multiwfn³ and VMD⁴.

References

- [S1] G. Sheldrick, *Acta Crystallogr., Sect. C: Struct. Chem.*, 2015, **71**, 3–8.
- [S2] M. J. Frisch, G. W. Trucks, H. B. Schlegel, G. E. Scuseria, M. A. Robb, J. R. Cheeseman, G. Scalmani, V. Barone, B. Mennucci, G. A. Petersson, H. Nakatsuji, M. Caricato, X. Li, H. P. Hratchian, A. F. Izmaylov, J. Bloino, G. Zheng, J. L. Sonnenberg, M. Hada, M. Ehara, K. Toyota, R. Fukuda, J. Hasegawa, M. Ishida, T. Nakajima, Y. Honda, O. Kitao, H. Nakai, T. Vreven, J. A. Montgomery, Jr, J. E. Peralta, F. Ogliaro, M. Bearpark, J. J. Heyd, E. Brothers, K. N. Kudin, V. N. Staroverov, R. Kobayashi, J. Normand, K. Raghavachari, A. Rendell, J. C. Burant, S. S. Iyengar, J. Tomasi, M. Cossi, N. Rega, N. J. Millam, M. Klene, J. E. Knox, J. B. Cross, V. Bakken, C. Adamo, J. Jaramillo, R. Gomperts, R. E. Stratmann, O. Yazyev, A. J. Austin, R. Cammi, C. Pomelli, J. W. Ochterski, R. L. Martin, K. Morokuma, V. G. Zakrzewski, G. A. Voth, P. Salvador, J. J. Dannenberg, S. Dapprich, A. D. Daniels, O. Farkas, J. B. Foresman, J. V. Ortiz, J. Cioslowski and D. J. Fox, Gaussian 09, Revision D.01, Gaussian, Inc., Wallingford, CT, 2009.
- [S3] T. Lu; F. Chen, Multiwfn: A multifunctional wavefunction analyzer. *J. Comput. Chem.*, 2012, **33**, 580-592
- [S4] W. Humphrey; A. Dalke; K. Schulten, VMD: Visual molecular dynamics. *J. Mol. Graph.*, 1996, **14**, 33-38.

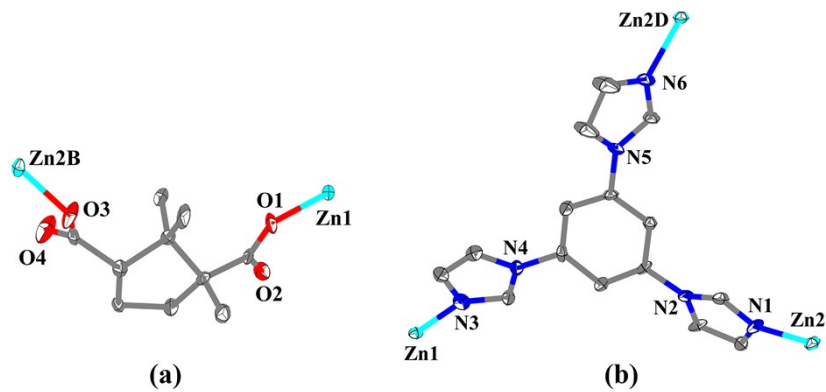


Figure S1. The coordination modes of D-Cam (a) and tib (b).

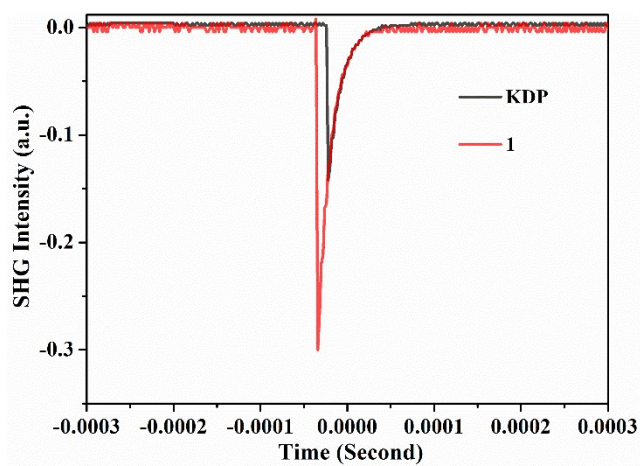


Figure S2. Oscilloscope traces of SHG signals of KDP and 1.

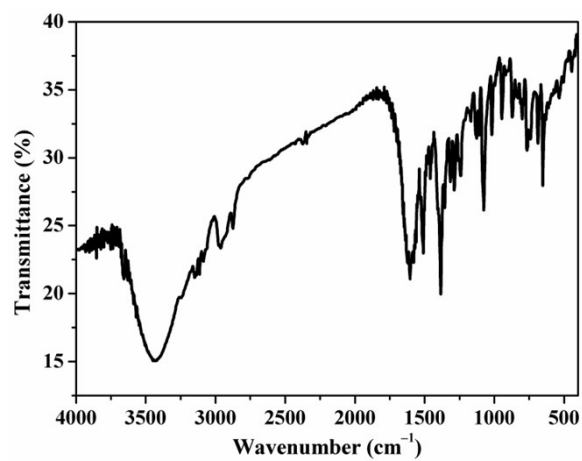


Figure S3. IR plot of 1.

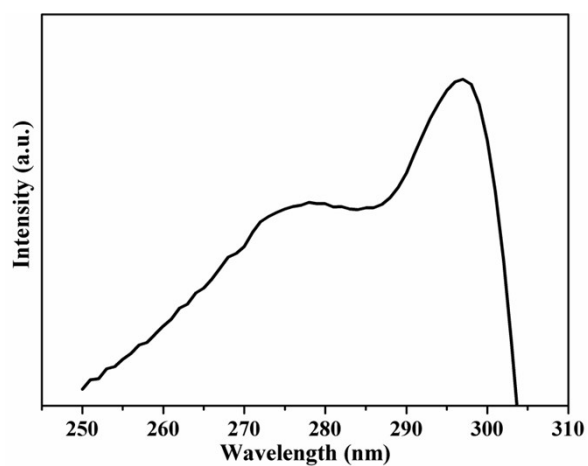


Figure S4. The prompt excitation spectra of **1** at room temperature.

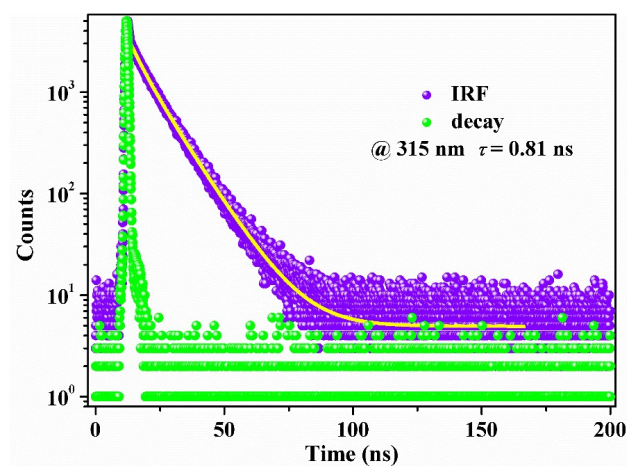


Figure S5. The decay and IRF spectra of **1**.

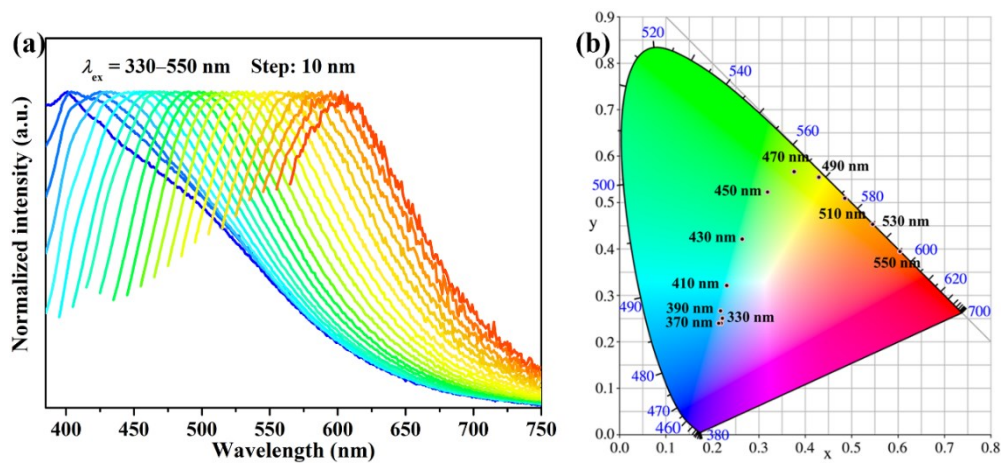


Figure S6. The PL spectra (a) and CIE coordinate (b) of **1** at room temperature.

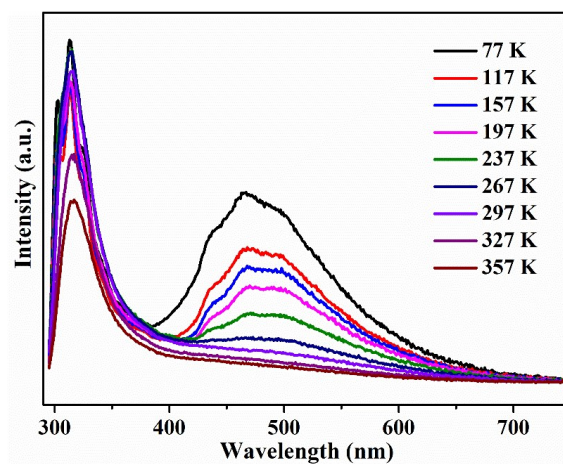


Figure S7. The temperature-dependent emission spectra of **1**.

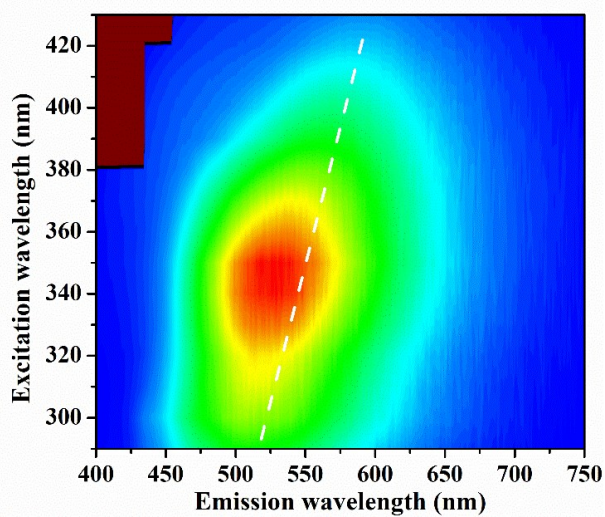


Figure S8. The excitation wavelength-dependent emission spectra.

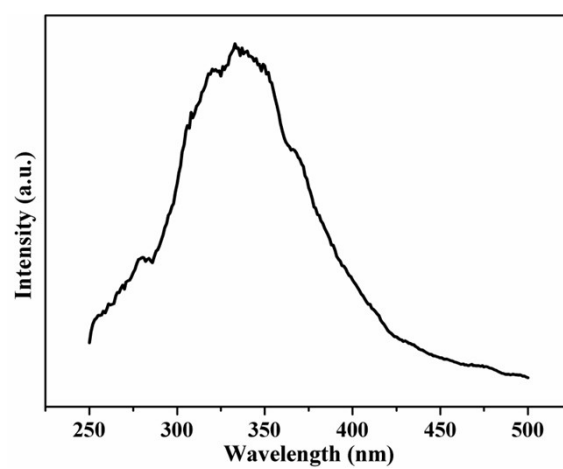


Figure S9. The delayed excitation spectra of **1** at room temperature.

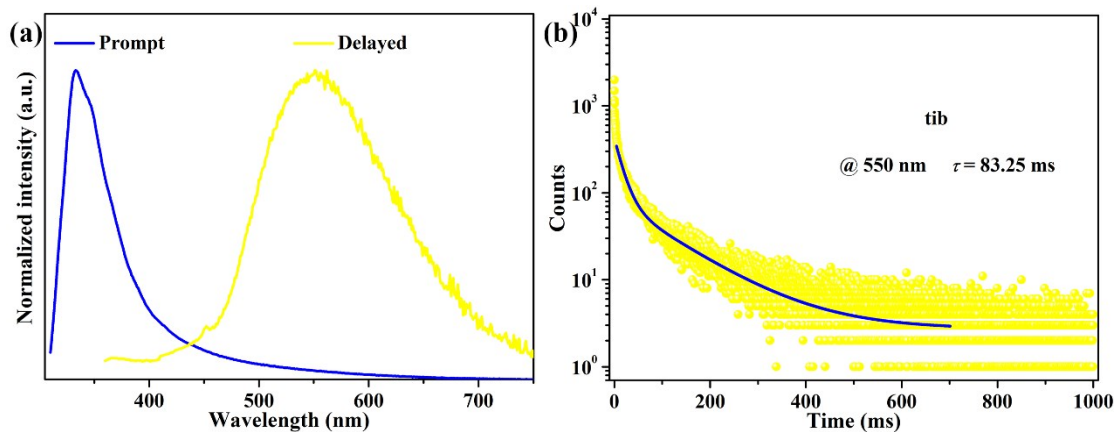


Figure S10. (a) Prompt and delayed PL emission spectra of tib ($\lambda_{\text{ex}} = 307$ nm, 380 nm). (b) PL decay and fit curves obtained at room temperature.

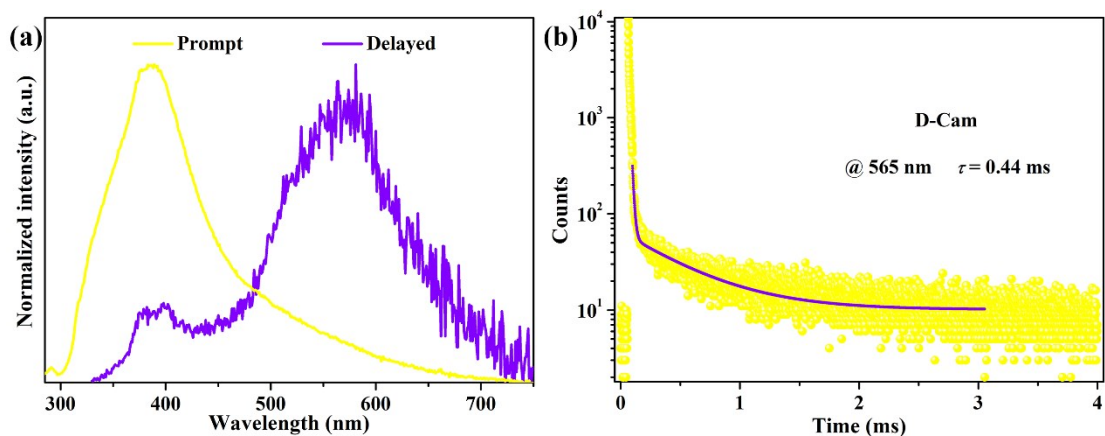


Figure S11. (a) Prompt and delayed PL emission spectra of **D-Cam** ($\lambda_{\text{ex}} = 267$ nm, 310 nm). (b) PL decay and fitting curves obtained at room temperature.

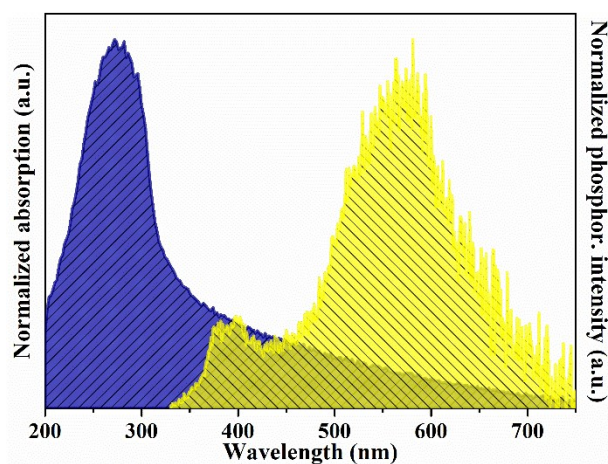


Figure S12. Normalized phosphorescence spectrum of **D-Cam** and absorption spectrum of **tib**.

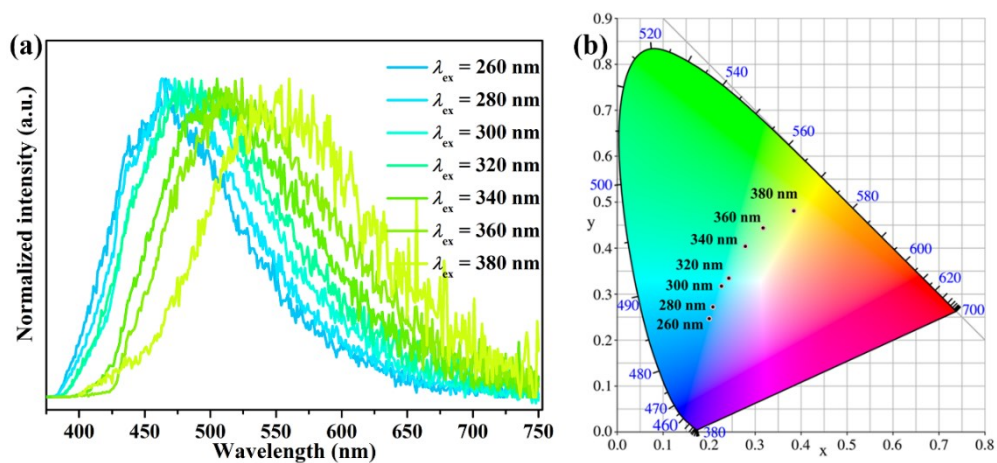


Figure S13. The delayed emission spectra (a) and CIE coordinate (b) of **1** at 77 K.

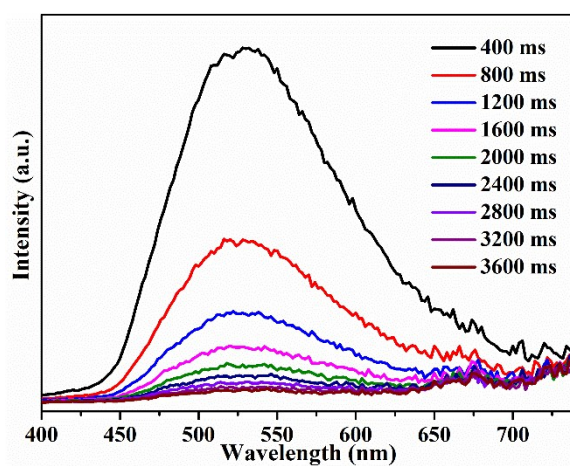


Figure S14. Time-resolved emission spectra ($\lambda_{ex} = 333$ nm).

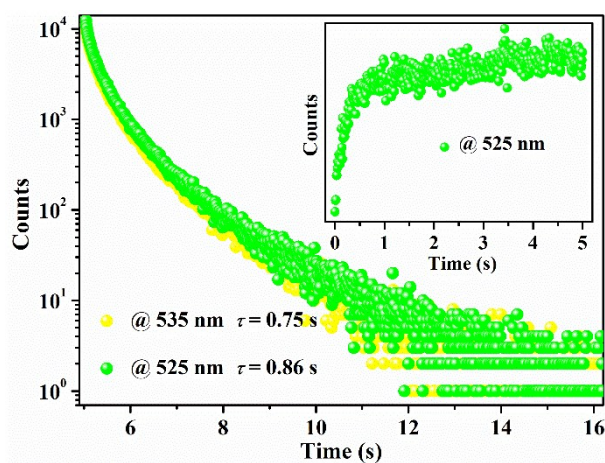


Figure S15. (a) RTP decay at 525 nm and 535 nm of **1** (Insert: photo-activable process).

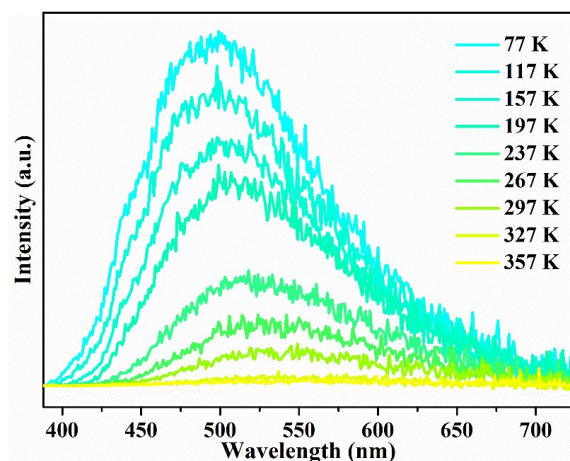


Figure S16. The temperature-dependent emission spectra ($\lambda_{\text{ex}} = 333\text{nm}$).

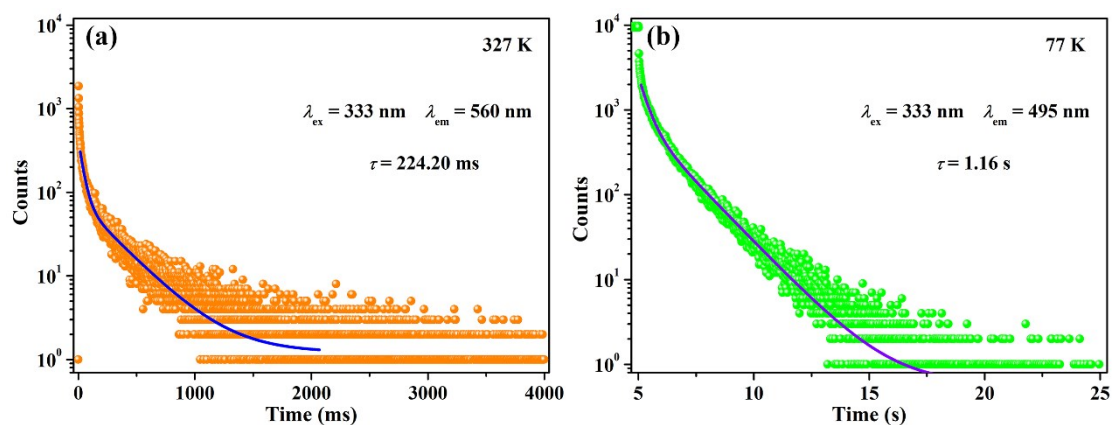


Figure S17. (a) PL decay and fitting curves obtained at 77 K and (b) 327 K.

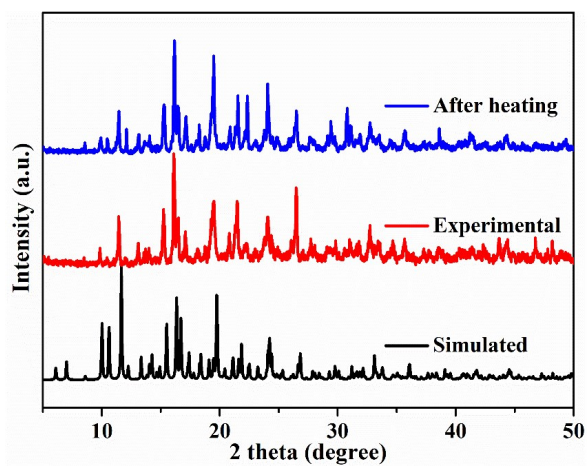


Figure S18. PXRD and simulated profiles of **1**.

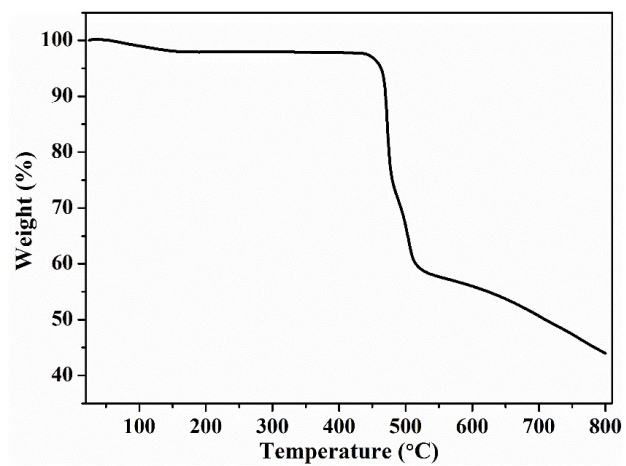


Figure S19. TG profile of 1.

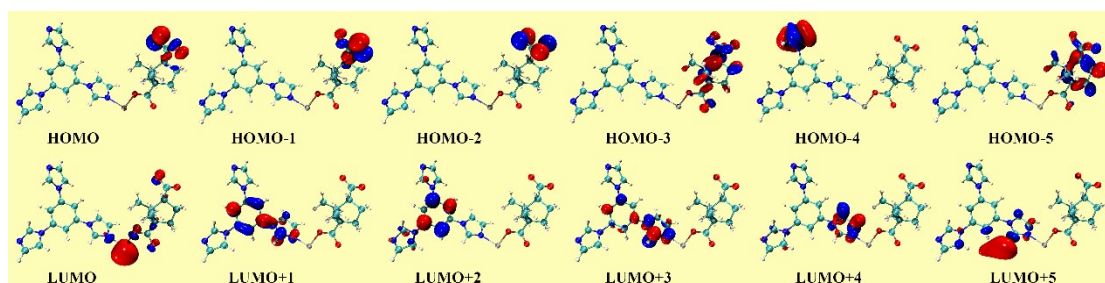


Figure S20. Calculated molecular orbitals.

Table S1. Crystallographic data for **1** at 100K

| | 1 | |
|---|---|--------|
| Formula | C ₆₀ H ₇₀ N ₁₂ O ₁₄ Zn ₃ | |
| Mr (g·mol ⁻¹) | 1379.39 | |
| Space group | P2 ₁ 2 ₁ 2 | |
| Crystal system | Orthorhombic | |
| <i>a</i> (Å) | 17.6445(2) | |
| <i>b</i> (Å) | 25.2002(3) | |
| <i>c</i> (Å) | 6.87410(10) | |
| <i>V</i> (Å ³) | 3056.53(7) | |
| <i>Z</i> | 2 | |
| <i>F</i> (000) | 1432 | |
| <i>D_c</i> (gcm ⁻³) | 1.499 | |
| <i>μ</i> (mm ⁻¹) | 2.005 | |
| <i>R</i> _{int} | 0.0293 | |
| | -21 ≤ <i>h</i> ≤ 21 | |
| limiting indices | -30 ≤ <i>k</i> ≤ 21 | |
| | -8 ≤ <i>l</i> ≤ 8 | |
| Collected reflections | 21484 | |
| Unique reflections | 5930 | |
| GOF on <i>F</i> ² | 1.039 | |
| <i>R</i> ₁ , <i>wR</i> ₂ [<i>I</i> > 2σ(<i>I</i>)] | 0.0581 | 0.1560 |
| <i>R</i> ₁ , <i>wR</i> ₂ [all data] | 0.0588 | 0.1568 |

$${}^a R_1 = \sum \frac{\|F_o\| - |F_c|}{\sum |F_o|} \quad {}^b wR_2 = \left\{ \frac{\sum [w(F_o^2 - F_c^2)^2]}{\sum w(F_o^2)^2} \right\}^{1/2}.$$

Table S2. Selected bond lengths (Å) and angles (°) for **1** at 100 K

| 1 | | | |
|---------------------|----------|---------------------|-----------|
| Zn(1)-O(1) | 1.943(5) | Zn(2)-O(5A) | 1.965(10) |
| Zn(1)-O(1)#1 | 1.943(5) | Zn(2)-O(5) | 2.020(12) |
| Zn(1)-N(3) | 2.046(5) | Zn(2)-N(1) | 2.021(5) |
| Zn(1)-N(3)#1 | 2.046(5) | Zn(2)-N(6)#3 | 2.024(6) |
| Zn(2)-O(3)#2 | 1.940(5) | Zn(2)-O(6A) | 2.334(10) |
| O(1)-Zn(1)-O(1)#1 | 121.3(3) | O(5A)-Zn(2)-N(1) | 109.2(3) |
| O(1)-Zn(1)-N(3) | 90.8(2) | O(5)-Zn(2)-N(1) | 104.6(3) |
| O(1)#1-Zn(1)-N(3) | 116.3(2) | O(3)#2-Zn(2)-N(6)#3 | 99.0(3) |
| O(1)-Zn(1)-N(3)#1 | 116.3(2) | O(5)-Zn(2)-N(6)#3 | 122.8(4) |
| O(1)#1-Zn(1)-N(3)#1 | 90.8(2) | N(1)-Zn(2)-N(6)#3 | 103.6(2) |
| N(3)-Zn(1)-N(3)#1 | 124.5(3) | O(3)#2-Zn(2)-O(6A) | 87.6(3) |
| O(3)#2-Zn(2)-O(5A) | 114.5(3) | O(5A)-Zn(2)-O(6A) | 60.2(4) |
| O(3)#2-Zn(2)-O(5) | 101.9(4) | N(1)-Zn(2)-O(6A) | 89.1(3) |
| O(3)#2-Zn(2)-N(1) | 127.0(2) | N(6)#3-Zn(2)-O(6A) | 157.4(3) |

Symmetry codes: #1: -x+1, -y+2, z; #2: -x+3/2, y-1/2, -z+1; #3: x-1/2, -y+3/2, -z; #4: -x+1, -y+1, z; #5: x+1/2, -y+3/2, -z; #6: -x+3/2, y+1/2, -z+1.

Table S3 Phosphorescence lifetimes (τ) of **1**.

| Compound | Temperature | Wavelength (nm) | Excitation light | τ_1 (ms) | A_1 (%) | τ_2 (ms) | A_2 (%) | $\langle\tau\rangle$ (ms) | χ^2 |
|--------------|-------------|--------------------|---------------------|------------------|--------------|------------------|--------------|------------------------------|----------|
| 1 | RT | 525 | uF2 | 150.2 | 34.72 | 701.4 | 65.28 | 510.0 | 1.260 |
| | | 525 | Xe | 405.2 | 47.72 | 1270 | 52.28 | 857.3 | 1.217 |
| | | 535 | Xe | 343.8 | 50.62 | 1162 | 49.38 | 747.8 | 1.230 |
| | 327 K | 550 | uF2 | 40.24 | 30.28 | 304.1 | 69.72 | 224.2 | 1.176 |
| | 77 K | 495 | uF2 | 373.0 | 32.87 | 1540 | 67.13 | 1156.4 | 1.147 |
| tib | RT | 550 | uF2 | 16.93 | 34.19 | 117.7 | 65.81 | 83.2 | 1.237 |
| D-Cam | RT | 565 | uF2 | 0.014 | 14.16 | 0.502 | 85.84 | 0.44 | 1.141 |

$\langle\tau\rangle = \sum A_j \tau_j^2 / \sum A_j \tau_j$, $j=1, 2, 3, \dots$; RT = Room temperature.